INTERNATIONAL JOURNAL OF CLIMATOLOGY
Int. J. Climatol. 19: 1–26 (1999)

ASSESSING SIMULATIONS OF DAILY TEMPERATURE AND PRECIPITATION VARIABILITY WITH GLOBAL CLIMATE MODELS FOR PRESENT AND ENHANCED GREENHOUSE CLIMATES

K. McGUFFIE[a,*], A. HENDERSON-SELLERS[b], N. HOLBROOK[c], Z. KOTHAVALA[c], O. BALACHOVA[c] and J. HOEKSTRA[d]

[a] *Department of Applied Physics, University of Technology, Sydney, Australia*
[b] *Australian Nuclear Science and Technology Organisation, Sydney, Australia*
[c] *Climatic Impacts Centre, Macquarie University, Sydney, Australia*
[d] *KEMA, The Netherlands*

Received 10 December 1996
Revised 22 June 1998
Accepted 29 June 1998

ABSTRACT

The enhanced greenhouse climates of five different global climate models are examined with reference to the ability of the models to characterize the frequency of extreme events on both a regional and global scale. Ten years of model output for both control and enhanced greenhouse conditions are utilized to derive return periods for extreme temperature and precipitation events and to characterize the variability of the model climate at both regional and global scales. Under enhanced greenhouse conditions, return periods for extreme precipitation events are shorter and there is a general increase in the intensity of precipitation and number of wet spells in most areas. There is a decrease in frequency of cold temperature extremes and an increase in hot extremes in many areas. The results show a reasonable level of agreement between the models in terms of global scale variability, but the difference between model simulations of precipitation on a regional scale suggests that model derived estimates of variability changes must be carefully justified. Copyright © 1999 Royal Meteorological Society.

KEY WORDS: general circulation models; NCAR community climate model; Australian BMRC model; temperature, extremes; rainfall, extremes; return periods; enhanced greenhouse conditions; rain days; dry spells

1. GREENHOUSE CHANGE AND CLIMATIC VARIABILITY

It is now well known that concentrations of greenhouse gases in the atmosphere have been increasing since the mid 19th century as a result of human activities. Current concern is that these increased concentrations of gases could result in global and regional climatic changes (Houghton *et al.*, 1990, 1996). The impacts of this enhanced greenhouse are not yet fully understood and may depend upon both the degree and the speed of this climatic change. Still more importantly, it is now widely recognized that changes in the number, frequency or intensity of extreme climatic events are likely to have a much greater impact on natural and human systems than small shifts in the mean values (Tegart *et al.*, 1990). Extreme events, such as floods, droughts and 'heatwaves' are a major trigger for public concern about climate issues. Despite the need for information on such events, it has been difficult to gather meaningful information about the likely impact of enhanced greenhouse gases on the frequency of extremes and the variability of important climate parameters. Recent regional studies (Hu *et al.*, 1998; Karl and Knight, 1998) have suggested that heavy precipitation events have become more common in the United States, but global scale information is difficult to obtain.

* Correspondence to: Department of Applied Physics, University of Technology, Sydney PO Box 123, Broadway NSW 2007, Australia; fax: +61 3 9669 4660; e-mail: k.mcguffie@bom.gov.au

Contract grant sponsor: Model Evaluation Consortium for Climate Assessment; the Department of the Environment, Sport and Territories; the Australian Research Council

CCC 0899–8418/99/010001–26$17.50

The global climate model (GCM) is generally portrayed as the most useful tool with which to investigate likely future climatic changes. However, there are many reasons why the results from such computer-based models must be treated with caution. Climate models still fail to reproduce the present-day climate in a fully satisfactory way and large uncertainties remain in the simulation of cloud, ocean- and land-surface moisture processes. Climate models also differ from one another in their representation of both the present-day climate and future greenhouse-warmed climates. In addition to these general caveats, it must be noted that the results described here are from simulations performed in 1992 as part of the Model Evaluation Consortium for Climate Assessment (MECCA) project (Henderson-Sellers *et al*., 1995). The results displayed here are from equilibrium (not transient) simulations with models which do not include fully three-dimensional oceans. The models all have simple thermodynamic sea-ice models and most have simple (bucket) land-surface schemes. None incorporate the effects of sulphate aerosols. Even though this paper does not represent 'state-of-the-art' results, it does display climates (present and future) from a group of recent climate models. The data presented, therefore, offer an assessment of the level of agreement among one subset of the 30–40 global climate models currently employed worldwide (Gates, 1992).

While specific case studies should use the most up-to-date and most completely validated model results available, anyone using results from one particular climate model must recognize that it is only one view of the future. Results from one model will not represent the range of possible outcomes, nor will it represent the full complexity and uncertainty associated with future climatic prediction. This paper serves to put into context such single model evaluations and particularly the degree of uncertainty associated with current and future simulations of climatic variability and extremes.

Gordon *et al*. (1992) investigated changes in the frequency of simulated daily rainfall. Whetton *et al*. (1993) noted that the frequency distribution of daily rainfall may change significantly, with a marked increase in heavy rainfall days. Katz and Brown (1992) have demonstrated that a change in the variance can have a larger impact on the number of threshold exceedances and the exceedance frequencies for monthly maxima than a change in mean values, while Mearns *et al*. (1995a), Mearns *et al*. (1995b) have more recently stressed the importance of changes in daily variability and higher order statistics for climate impact assessment. Impacts and policy assessments are demanding more information from climate modellers. Natural and human systems are also affected by changes in day-to-day extremes.

Extreme weather events occur at synoptic or smaller scales. Evaluation of likely extreme events must await very much higher resolution GCMs or make use of embedded regional models or some other type of downscaling technique (Brown and Katz, 1995). They are not captured by current coarse resolution GCMs since the spectral cut-off affects the dynamics around the cut-off scale (Roeckner and von Storch, 1980), the surface orographic and land-type features are not represented (Giorgi and Mearns, 1991) and the dynamic features of importance (e.g. intense convective activity in thunderstorms and tropical cyclones) are not represented (Lighthill *et al*., 1994; Henderson-Sellers *et al*., 1998).

This paper assesses the level of agreement which exists among five GCM representations of daily climatic 'variability' and 'frequency of extremes' as represented by the two most important and readily recognized parameters: surface temperature and precipitation. This is a worthwhile assessment because model uncertainty is not confined to mean climates; some previous assessments of climatic change have focused on extreme events and have assumed that the variability underlying these events does not change (Whetton *et al*., 1993; Hennessey and Pittock, 1995) and increased interest in downscaling has, so far, neglected the degree of uncertainty in simulated variability and higher order statistics.

2. MODELS EMPLOYED AND CLIMATIC VARIABLES ASSESSED

This paper evaluates the temperature and precipitation variability as archived in a database of daily results established by the MECCA analysis team (Henderson-Sellers *et al*., 1995) from five of the MECCA Phase 1 experiments that prescribed a variety of enhanced greenhouse gas concentrations. The MECCA project was designed to assess the reliability of GCMs as a means of quantifying the probable range of

future climatic change and hence uncertainty and to convey the resulting information to policy-makers and other interested organizations and concerned individuals (Henderson-Sellers *et al.*, 1995).

The five models analyzed in this paper (Table I) are: CCM0, a highly modified version of NCAR's (National Center for Atmospheric Research) community climate model (CCM) Version 0; CCM1Oz, CCM1W and CCM1, being three different versions of CCM version 1; and BMRC, the model of the Australian Bureau of Meteorology Research Centre. It should be noted that the control run and the perturbed run are not the same for all of the models. CCM1W incorporates the effect of all the greenhouse gases. The other models use CO_2 as the sole greenhouse gas with a concentration of 330 ppmv in the control run. CCMl's perturbed simulation uses 460 ppmv CO_2, whereas the other models have $2 \times CO_2$ (660 ppmv) in their perturbed run. The enhanced greenhouse gas results are derived from experiments in which an instantaneous increase of trace gases was imposed and the model climate allowed to come into equilibrium. All models employ a mixed layer ocean of 50 m depth. CCM0 and CCM1 do not include a q-flux correction. Two schemes are used to calculate convection: moist convective adjustment (Manabe *et al.*, 1965) for CCM1Oz, CCM1W and CCM1 and penetrative convection (Kuo, 1974) for CCM0 and BMRC. The two convective schemes have been compared by Tiedtke (1984). The penetrative convection scheme's distribution of the heating shows more agreement with observations.

Table I gives specific information about the models and experiments together with summary information on the results of the enhanced greenhouse runs. For all the models. the final 10 years of the control (present-day climate simulation) and the enhanced greenhouse climate simulation are used. The problem of validation of model climates is addressed extensively by the individual model developers listed in Table I and intercomparisons such as AMIP (Gates, 1992) provide information on model performance.

Table I. Characteristics of the climate models used in this study

	CCM1Oz	BMRC	CCM1W	CCM1	CCM0
Horizontal resolution	R15	R21	R15	R15	R15
Diurnal cycle	Yes	Yes	No	No	No
Control CO_2 (ppmv)	330	330	354+	330	330
Perturbed CO_2 (ppmv)	660	660	539	460	660
Land-surface scheme	BATS	Bucket	Bucket	Bucket	Bucket
Mixed layer depth (m)	50	50	50	50	50
Flux correction scheme	Yes	Yes	Yes	No	No
Convection scheme	MCA	PC	MCA	MCA	PC
Cloud scheme	RH	RH	RH	RH	RH
Cloud properties	fixed	fixed	fixed	fixed	fixed
Sea-ice layers	3	1	2	3	1
Perturbation ΔT (K)	2.53	2.14	4.00	2.97	4.52
Perturbation ΔP (%)	5.9	2.6	7.7	4.1	4.6
JJA ΔP (%)	5 7	1.6	6.9	5.5	5.5
DJF ΔP (%)	6.1	3.1	7.8	5.6	5.8
Reference	Henderson-Sellers *et al.* (1993)	Hart *et al.* (1990)	Wang *et al.* (1992)	Oglesby and Saltzman (1992)	Washington and Meehl (1992)

+, indicates trace gases (N_2O, CH4, CFC11, CFC12); mlo, mixed layer ocean; MCA, moist convective adjustment; PC, penetrative convection; RH, relative humidity based cloud.

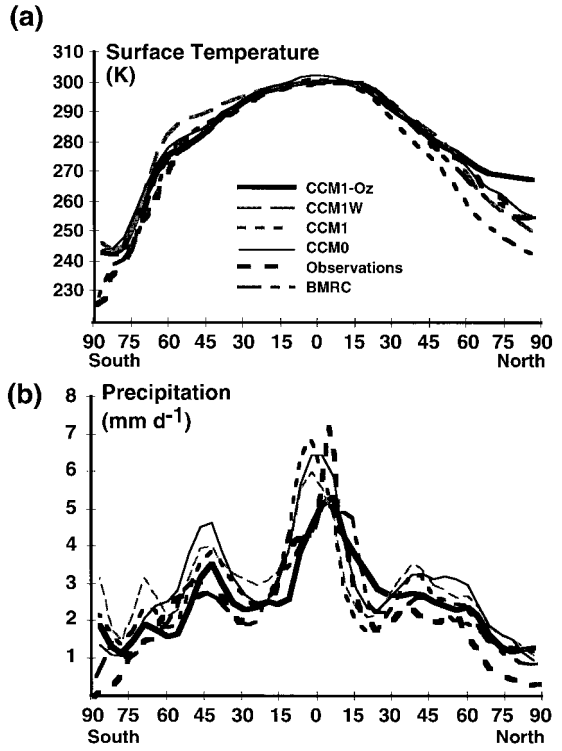

Figure 1. Zonal distribution of (a) surface temperature, (b) precipitation, from CCM1Oz, BMRC, CCM1W, CCM1, CCM0

All models except the BMRC model are derivatives of either version 0 or version 1 of the National Center for Atmospheric Research's community climate model and, originally, CCM0 was itself developed from a global model constructed in BMRC. The models are all 'related' so that in some ways the comparisons are more restricted than those across all available GCMs (Houghton *et al.*, 1990, 1992; Gates, 1992) which means that the range of uncertainty may appear to be less than from the whole community. There are also, however, many differences between these models in terms of the length of runs and in the underlying physical parameterizations used. These differences in the models and in the experiments are important and they will affect the level of agreement between the models. Moreover, there now exist other types of models, e.g. fully three-dimensional ocean models coupled to atmospheric models, and other types of experiments, e.g. transient increases in greenhouse gas amounts and those including the effects of increased sulphate aerosols, which produce notably different results (Houghton *et al.*, 1992; Penner and Taylor, 1994). The models used to generate the results analyzed here are coarse resolution (typically *ca.* 500 × 500 km 'grid-points') global models and for this and other reasons, their representation of regional-scale geography and climate is approximate. This lack of skill or agreement at the regional scale is a recognized difficulty with results from existing GCMs (Houghton *et al.*, 1996). All of the models (except BMRC) have been integrated at a spatial resolution of 4.5° latitude × 7.5° longitude. The BMRC model has a grid resolution of 3.3° latitude × 5.6° longitude.

An indication of the overall performance of the models is given in Figure 1 which shows the zonally and annually averaged precipitation and surface air temperature for the control run (present-day climate) of the five models and for observations (Legates and Willmott, 1990a,b). The model simulations agree reasonably with the observations but the precipitation maxima in the temperate zone are too high and the peak in the Intertropical Convergence Zone (ITCZ) is either slightly shifted to the south or underestimated. More detailed evaluations of intermodel differences form part of AMIP (Gates, 1992).

The global average precipitation and air temperature change for the models by season is also shown in Table I. All the models agree on an increase in average precipitation in both December–January–Febru-

ary (DJF) and June–July–August (JJA) with a larger change in the Northern Hemisphere winter (DJF). Interestingly, the model that has a smaller increase in CO_2 (to 460 ppmv) in the perturbed run, CCM1, shows about as much or more average change as the four other models.

3. DAILY VARIABILITY OF PRESENT-DAY AND ENHANCED GREENHOUSE SIMULATIONS

A number of different methods for illustrating the daily variability of model results are presented here. The variability can be thought of in terms of the standard deviation (S.D.) of all the daily values for a particular month over the 10 years, and can also be thought of as a measurement of the smoothness of the temperature time series (represented here by its second time derivative).

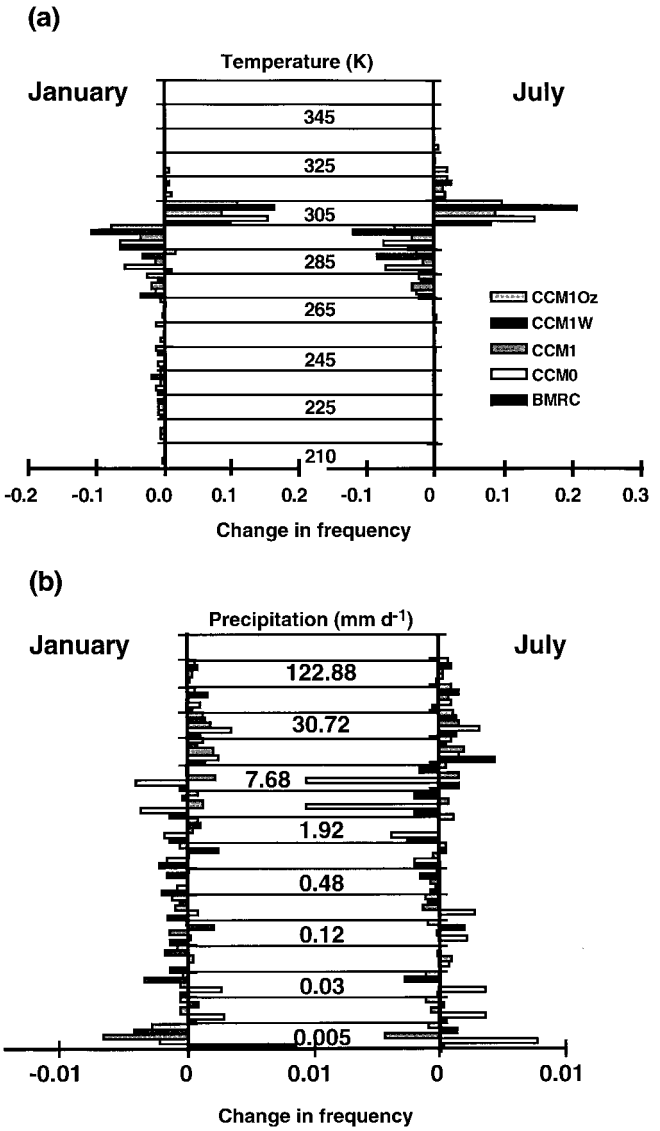

Figure 2. Changes in area weighted frequency distributions for January and July for (a) surface temperature and (b) precipitation from CCM1Oz, BMRC, CCM1W, CCM1, CCM0. Each 'bin' has five bars presented in the order shown in the key

Figure 2 shows the way in which the global frequency distribution of temperature and precipitation respond to increased CO_2. Daily occurrences of temperature at each grid-point within a 1.0°C interval, centered at the indicated temperature were computed and area weighted. For precipitation (Figure 2(b)), the amounts in successive categories increase exponentially. It is clear that there is general (but not complete) agreement between the models for the change in temperature frequency. There is a characteristic shift to higher temperatures in all models. In January, all models show a reduction in very cold areas, associated with the decrease in snow and ice area in the Northern Hemisphere winter (Henderson-Sellers and Hansen, 1995) which accompanies the enhanced CO_2. For all five models, there is an increase in the frequency of occurrence of more intense precipitation and some of the models show an increase in the frequency of less intense precipitation, consistent with an overall increase in precipitation upon which all the models agree. There is, however, very much less agreement between models for precipitation than for temperature. Although all models show a shift towards more extreme precipitation events there is less consensus in lighter precipitation regimes. This may be due to the confounding of changes in frequency and intensity of events at timescales finer than the daily scale considered here, meaning that conclusions from these results regarding increased frequency of droughts would be difficult to justify. It should be noted that most of the models predict decreases in the frequencies of middle precipitation categories.

4. GLOBAL DISTRIBUTION OF RETURN PERIODS FOR EXTREME EVENTS

The frequency of extreme events can be analyzed by considering the return period for events of various magnitudes. To enhance the analysis of changes induced in the model climates, this study follows the method of Hennessey *et al.* (1993) who showed similar changes in rainfall intensity through low- and mid-latitudes under enhanced greenhouse conditions among three different GCMs. Fowler and Hennessey (1995) showed the possibility of substantial increases in the frequency and magnitude of extreme daily precipitation under enhanced greenhouse conditions. In this section, extreme precipitation and temperature events are examined at the resolution of the GCM.

There is no universal threshold which can be considered extreme for either temperature or precipitation. Such factors are geographically varying and also influenced the level of adaptation. Heavy rainfall is analyzed here in terms of the ranges 10–20, 20–40, 40–80 mm day^{-1} and >80 mm day^{-1}.

In this section, the average return period for precipitation of more than 40 mm day^{-1} over 10 years is analyzed for the five models. Figure 3(a) shows the return period of precipitation between 40 and 80 mm day^{-1} for the control simulation. The darker shades show areas where such extreme events occur very frequently. There are, loosely speaking, three areas of intense rainfall in tropical regions, over the Amazon, tropical Africa and Southeast Asia. There is substantial variation between the model derived distributions of return periods for extreme events. The contrast between the convective regions of the tropics and the subtropical high pressure areas is good in CCM0 and the BMRC, but CCM1W does not have the same differentiation of these regions. The level of agreement for events >80 mm day^{-1} is slightly better, although the BMRC model produces notably fewer of these very extreme events. The contrast in model performance in the eastern Pacific can possibly be attributed to the different performance of the mixed layer ocean schemes. Different schemes reproduce the SST spatial variation with various levels of success.

Extremes of temperature have an impact on human health through interactions with air quality in all societies, and on energy demand in technologically dependent societies. All five models agree on the existence of extremely cold temperatures (Figure 4(a)) over the polar regions and adjacent northern parts of Eurasia and northern America with a minimal return period (up to 4 days). CCM1Oz and CCM0 somewhat capture patterns of high frequency of extremely low temperatures in Siberia where mean observed temperatures for January are as low as -20 to -30°C, whereas the other three models have a uniform minimal return period throughout all northern regions of Eurasia. Those models also have a higher frequency (return periods can be as short as 4–16 days) of low temperature extremes over eastern and northern Europe (including Scandinavia), as they are generally cooler over these regions than

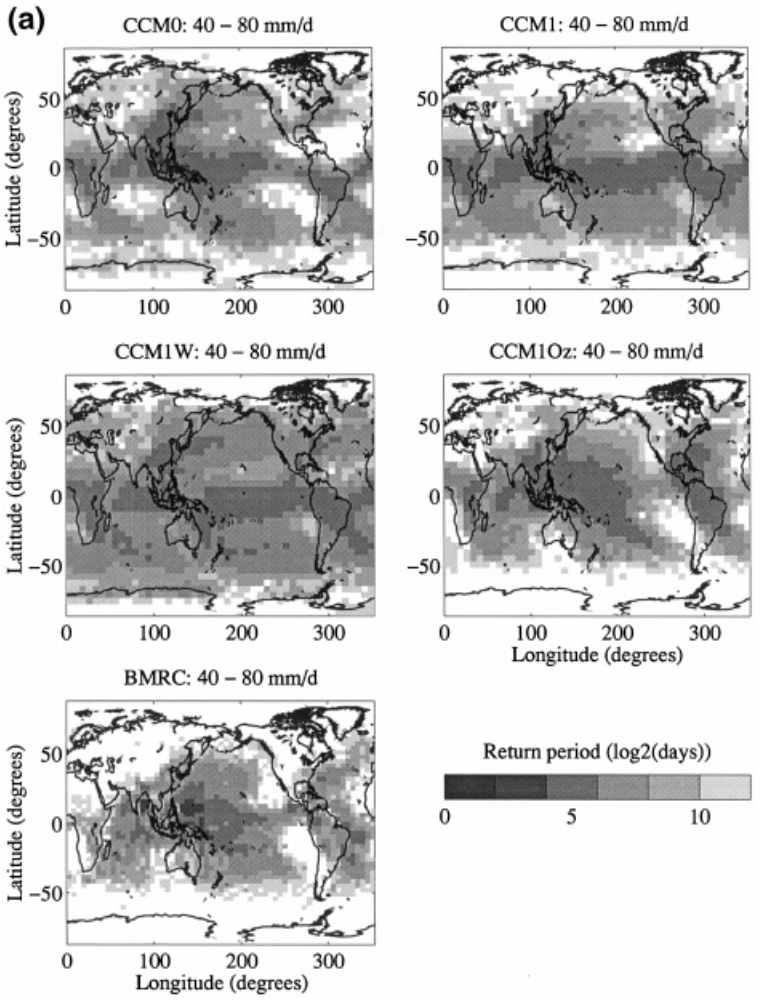

Figure 3. Return period of extreme precipitation for (a) between 40 and 80 mm day^{-1} and (b) greater than 80 mm day^{-1}. Return periods are in units of $\log_2$ of the number of days. Hence, 0 represents 1 day, 1 represents 2 days, etc.

CCM1Oz and CCM0. Interestingly, CCM1Oz shows a lower frequency of cold extremes (lower than -20 and $-20°$ to -10°C range) over the Arctic Ocean (16–64 days return period) which is in contrast with the rest of the models showing generally uniform return period 0–4 days for this region. This is consistent with the fact that CCM1Oz has significantly lower daily temperature S.D. and a higher mean temperature over the Arctic Ocean.

CCM0 has more 'hot' extremes in the control simulation than the other four models (Figure 4(b)). Extreme temperatures higher than 40°C are widely spread over all the continents. Highest frequency (0–16 days return periods) is found over large areas in Africa (Sahara and inner continental part south of the equator), Saudi Arabia, Middle East and Middle Asia, India and Southeast Asia. There are also large areas with a very high frequency (0–16 days return periods) of extremely high temperatures in South America, central and southern parts of the USA, and over almost all of the Australian continent. Two CCM1-type models (not CCM1Oz) show similar patterns of hot extremes across South America, but again, return periods are longer and areas are smaller compared to CCM0. Regions and frequency of extremes in CCM1Oz and BMRC models look fairly similar which may be directly attributable to the simulation of the diurnal cycle in these models. The other models do not incorporate the diurnal cycle and therefore simulate a quite different pattern of temperature extremes.

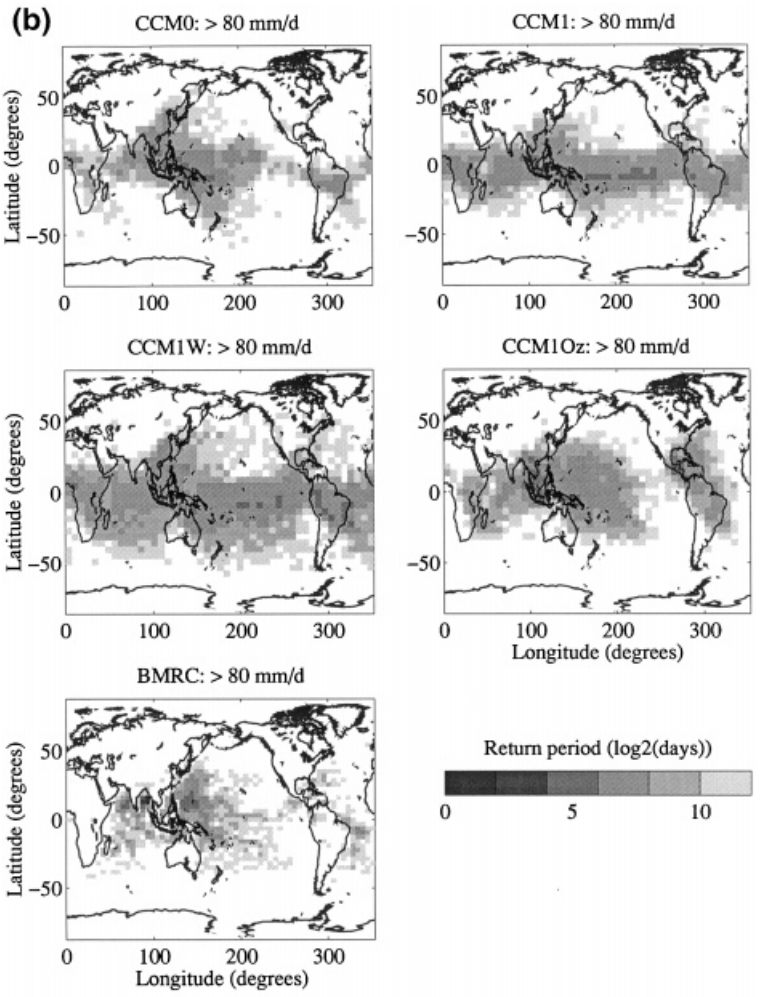

Figure 3 (*Continued*)

The surface temperature estimates from current climates given by the five GCMs under consideration have a number of deficiencies in relation to geographical distribution and magnitude of the surface temperature extremes. There are differences in the tropical and subtropical extreme temperature distribution, which may be directly related to the presence or absence of a diurnal cycle. Other regions are subject to the errors which are often correlated with errors in mean temperatures estimates, shown in Figure 1. However, frequency and geographical distribution of the temperature extremes seems to depend even more on the parameterization of the physical processes and the resolution of the models. CCM1Oz also includes an advanced land-surface parameterization scheme designed (Dickinson *et al.*, 1992) to incorporate the effects of vegetation on heat and moisture exchange between the land-surface and the atmosphere. Lack of global observations on temperature variability and extremes, as well as the relative newness of climate variability as an issue in climate modelling are major factors limiting reliability of GCM evaluation.

Under enhanced greenhouse conditions a notable decrease of cold temperatures frequency is shown in Canada, Alaska and northern parts of the USA (Figure 5(a)). There is also an overall decrease of frequency of cold extremes over western and northern parts of Russia (west of the Urals), and large parts of inner continental regions (e.g. China, Mongolia) and significantly longer return periods of extremely low temperatures in eastern Europe (100–144 days return periods compare to 16–36 days in the control

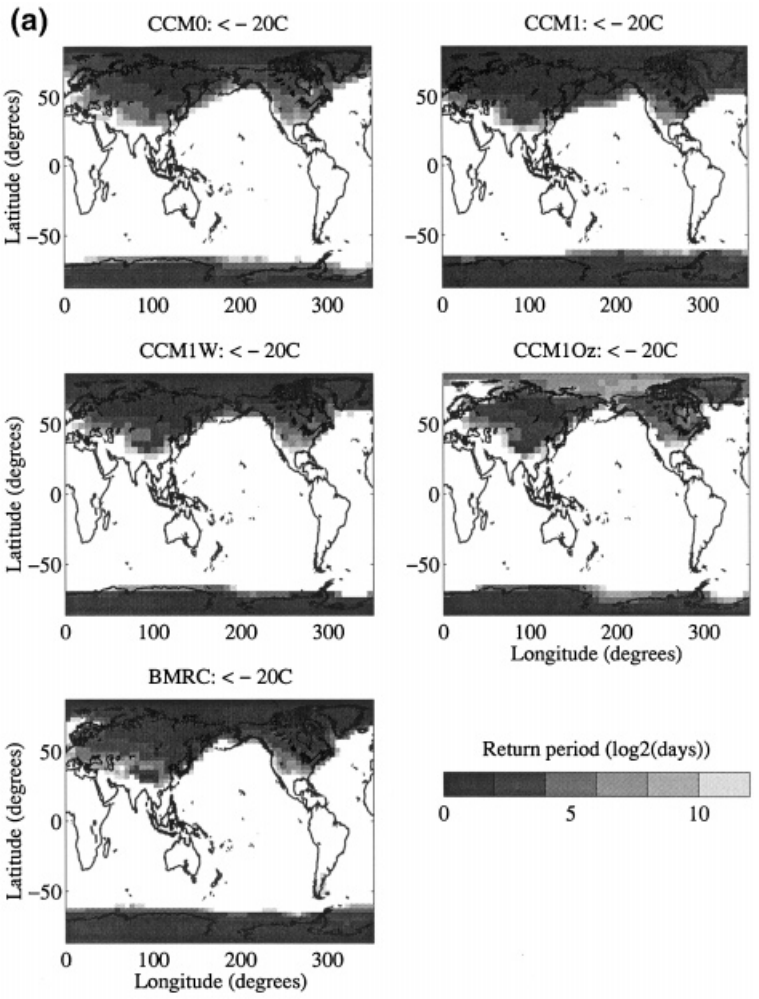

Figure 4. Return periods of extreme temperature for (a) less than -20 and (b) >40°C

simulation). This is consistent with a decrease in the area of snow cover in the marginal cryosphere region. There are some areas which show an increased frequency of cold events. This may be due, in the Northern Hemisphere, to an increase in the amount of snow at higher latitudes because of the increased precipitation.

There is a fair agreement amongst all the models concerning more frequent high temperature extremes over Australia and parts of Central North America (Figure 5(b)). However, particular locations of increases in hot extreme frequency vary. For example, CCM0 simulates shorter return periods of hot extremes only along the southeast coast of Australia whereas the other four models show similar changes of hot extreme frequency but in the inner parts of the continent. In Africa, all the models indicate decreases in the return periods for temperatures higher than $+40$°C. CCM1 and CCM1W show higher frequency over most of the continent, CCM1Oz and BMRC yield shorter return periods only in the regions north of the Equator including the Sahel (IPCC 3; see Section 5.1 for definition of IPCC regions). CCM0 shows an increase of hot extremes frequency almost everywhere but in the continental interiors. These areas show extreme high temperatures nearly all the time (Figure 4(b)) and as a result, further increase is impossible.

Other regions where most models agree upon an increase of hot extremes frequency are India (part of IPCC 2) and the Arabian Peninsula (CCM0 is an exception in both cases). Return periods for

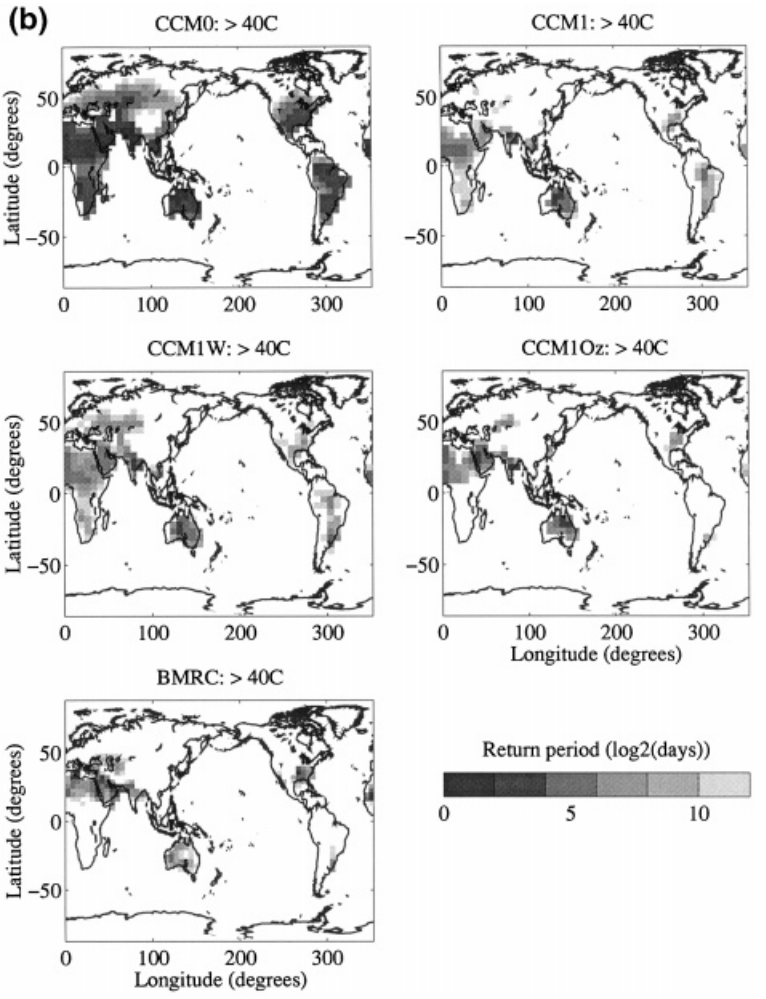

Figure 4 (*Continued*)

temperatures greater than $+40°C$ become shorter in CCM1W, CCM0 and BMRC enhanced greenhouse simulations over parts of IPCC 4 (Mediterranean countries and Southeast Europe) and also in South America (CCM1Oz, CCM1W and CCM0). Interestingly, most of the changes in higher temperature extremes are generally found over the regions where annually averaged temperatures do not change dramatically under enhanced greenhouse conditions (exceptions are Africa and Arabian Peninsula in CCM1 and CCM0 perturbed climates).

Figure 6(a) shows the change in return period for rainfall events between 40 and 80 mm day^{-1}. All models, with the possible exclusion of BMRC, agree to the increase in frequency of precipitation events between 40 and 80 mm day^{-1} in mid-latitudes. Most of the models also indicate an increase in frequency of very extreme precipitation events (> 80 mm day^{-1}) in the Intertropical Convergence Zone (Figure 6(b)), although consideration of the annual mean tends to smooth out the influence of the tropical convection. It is particularly clear that the patterns of change are associated with features of the general circulation. For example, the subtropical high pressure belts have a tendency to show reduced frequency of precipitation events between 40 and 80 mm day^{-1}, consistent with increased evaporation.

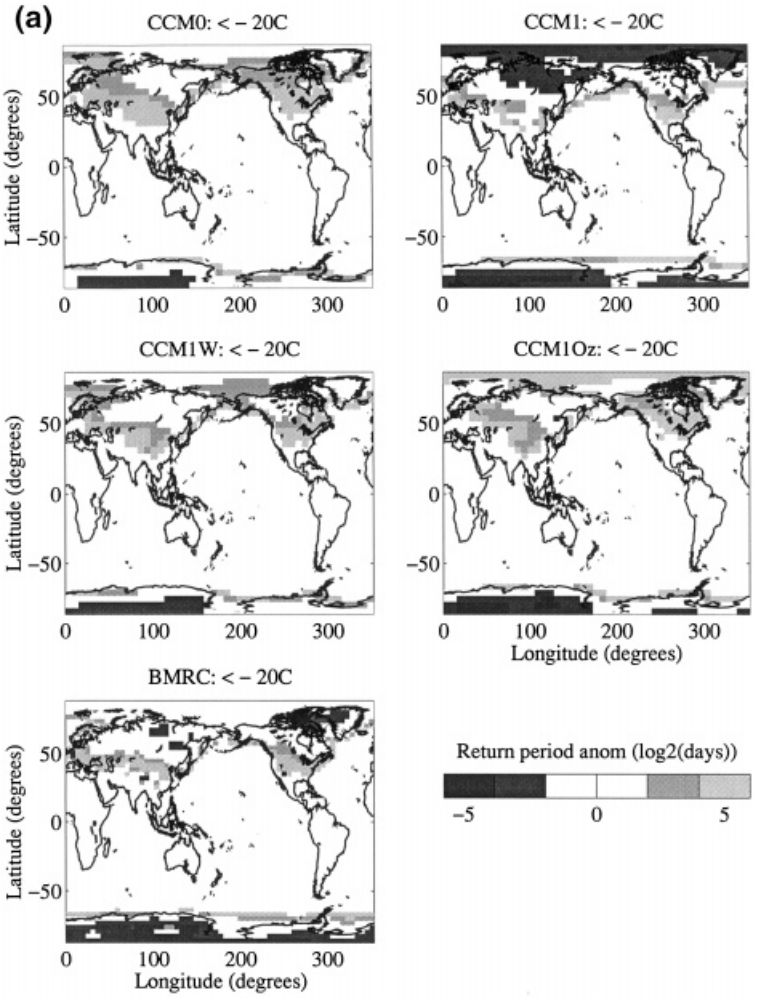

Figure 5. Changes in extreme temperature event return periods for (a) less than -20 and (b) >40°C

5. REGIONAL PRECIPITATION VARIABILITY

The increased radiative energy which impinges on the surface under enhanced greenhouse conditions is, in part, balanced by increased radiation and partly by increased latent heat fluxes. Houghton *et al.* (1990) anticipate an increase in convective rainfall, because this extra vertical heat transport needed to balance the radiative cooling of the atmosphere and radiative warming of the surface is most likely supplied by an increase of latent heat flux instead of sensible heat flux. The resulting increase in convective activity could lead to an increase in the frequency and intensity of heavy rainfall (Noda and Tokioka, 1989; Gordon *et al.*, 1992). Noda and Tokioka (1989) also observed a decrease in large scale stratiform rain which may decrease the number of rain-days at mid-latitudes. Parey (1994) however failed to find any significant change in the return period for heavy rainfall in three 30-year integrations for $1\times$, $2\times$ and $3\times CO_2$ conditions with the Laboratoire Météorologie Dynamique (LMD) GCM.

Droughts and floods affect agriculture not only because crops may suffer from water stress or too much soil water, but the ground may become so marshy that heavy machinery cannot be used for planting, maintaining and harvesting. The crucial scale for consideration of variability is the regional scale and in this section, the short-term variability of the regional precipitation is assessed for the five MECCA models under consideration. An estimate of this 'variability' which indicates the suddenness of changes in the

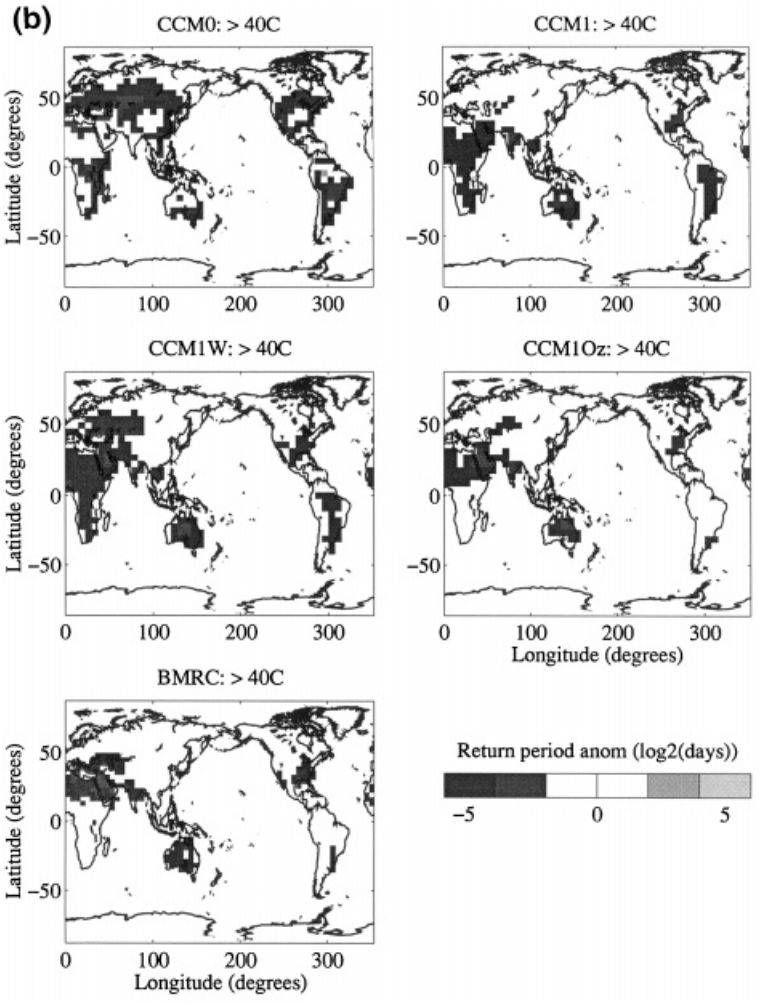

Figure 5 (*Continued*)

environment is derived here by applying the Laplacian operator to the mean annual time series of mean daily precipitation values. This variability is presented here as an absolute value. In one dimension (as here) the Laplacian reduces to the second derivative (d^2/dt^2).

5.1. Simulations of regional precipitation

Whetton *et al.* (1993) examined rainfall events in Australia in detail using the CSIRO model, with emphasis on floods and droughts. In the present study, the nature of precipitation variability is examined for the five IPCC regions (Houghton *et al.*, 1990): (i) Mid-West US (105–80°W, 35–50°N); (ii) South Asia (70–105°E, 5–30°N); (iii) the Sahel (20–40°E, 10–20°N); (iv) Southern Europe (10–45°E, 35–50°N); and (v) Australia (110–155°E, 45–12°S). The data presented here, except the number of rain-days and rainfall intensity, are extracted from the time series of area-averaged precipitation in each region. Although this area averaging will smooth out individual events, the inclusion of actual grid-point values, as if they were point station data is difficult to justify. The IPCC regions are not climatologically homogeneous and such averaging will inevitably obscure subregional phenomena. The level of confidence which might be attributed to such small scale features is unclear. The variability of precipitation is illustrated in Figure 7 for IPCC region 1 (North America). The figures show the actual ensemble mean daily precipitation series

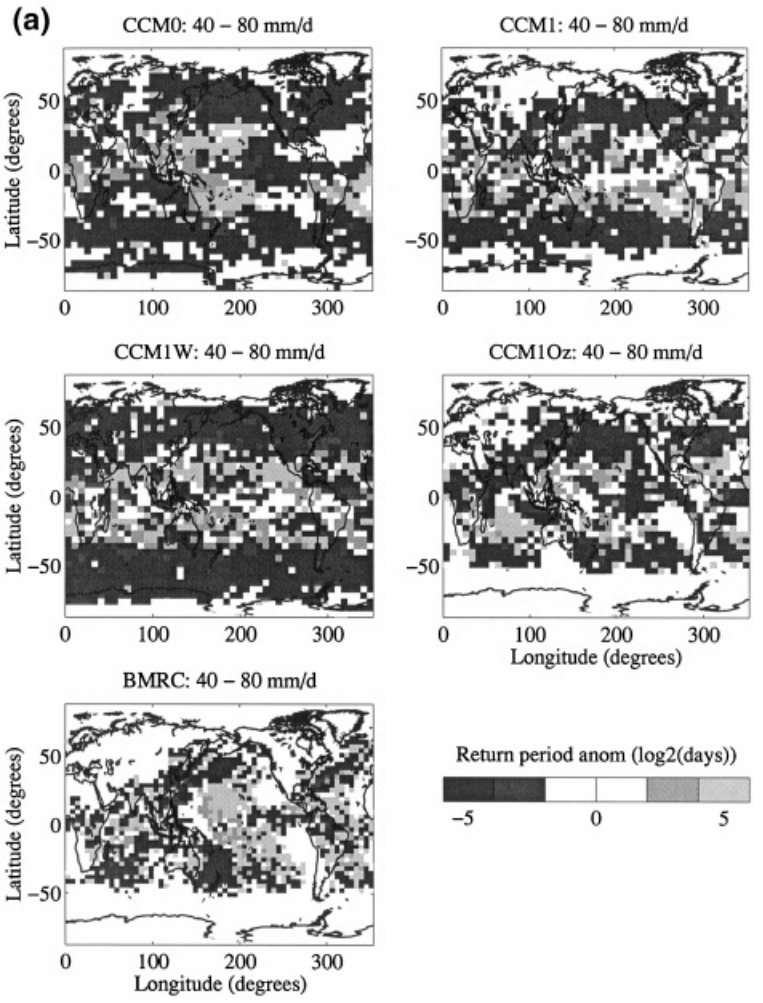

Figure 6. Changes in extreme precipitation event return periods for (a) between 40 and 80 mm day^{-1} and (b) greater than 80 mm day^{-1}

together with the Laplacian filtered series for both control and enhanced greenhouse ($|d^2/dt^2|$). It is clear that the magnitude of the variability as characterized by this particular measure differs between models. Some models have a very clear 'high variability' season (e.g. BMRC) whereas other models have a more constant pattern throughout the year (e.g. CCM1W). The character of the modeled seasonal cycles also varies between models. Two models, CCM0 and BMRC, display markedly different summer precipitation climates. The remaining models show climates in reasonable agreement with the observations, but do not display the same distribution of variability throughout the year. Table II shows the mean magnitude of the Laplacian filtered series for the five models for the five regions. At a regional scale, there is considerable disagreement in the nature of the variability change using this measure. Figure 8 shows the same quantities as Figure 7 but for the Australian region. The BMRC model gives an acceptable simulation of the annual cycle of Australian rainfall (dominated by summer monsoon rain) but there are substantial intermodel differences in variability for this region.

A useful way of studying the frequency distribution is examining the return period of events of a particular magnitude. However, the evaluation of return periods generated from such a short term record must be undertaken with care. It is important to recognize the increasing level of uncertainty associated with the return period of increasingly infrequent events. For example, an event which has a return period

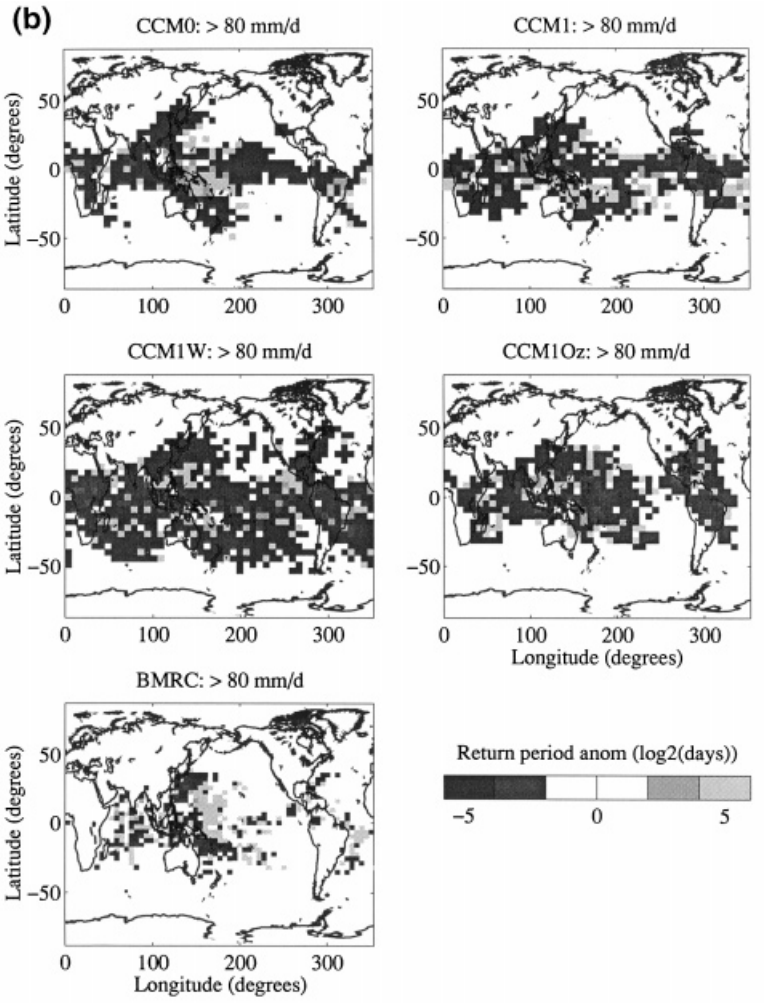

Figure 6 (*Continued*)

of 3650 days (10 years) will occur only once in the dataset and any predictions based on a single event would be rightly open to criticism. In an attempt to at least include a qualitative uncertainty in the assessment, an uncertainty based on the number of occurrences, n, in each category is included in this analysis such that the uncertainty, ε, is given by:

$$\varepsilon = \sqrt{1/n} \tag{1}$$

To assess the modeled changes in return period, the return periods for enhanced greenhouse conditions are presented as a ratio relative to the control conditions. For simplicity, the error bars in each case are derived from the average number of observations from all models with precipitation events of that magnitude and are limited to $+1$. The deviation indicated by this represents the magnitude of change which could be expected to occur at random given the average number of observations which are available in that category. Values of the ratio which are less than unity indicate that the modeled return period has decreased for precipitation events of a specified magnitude and values greater than one would likewise indicate a longer return period. Figure 9 shows the relative return period for enhanced CO_2 conditions for the five models in this study. The vertical columns show the relative return period for enhanced CO_2 and the lines show the bounds of the likely confidence, according to Equation (1). Although the number of observations is insufficient for a clear indication of return period changes,

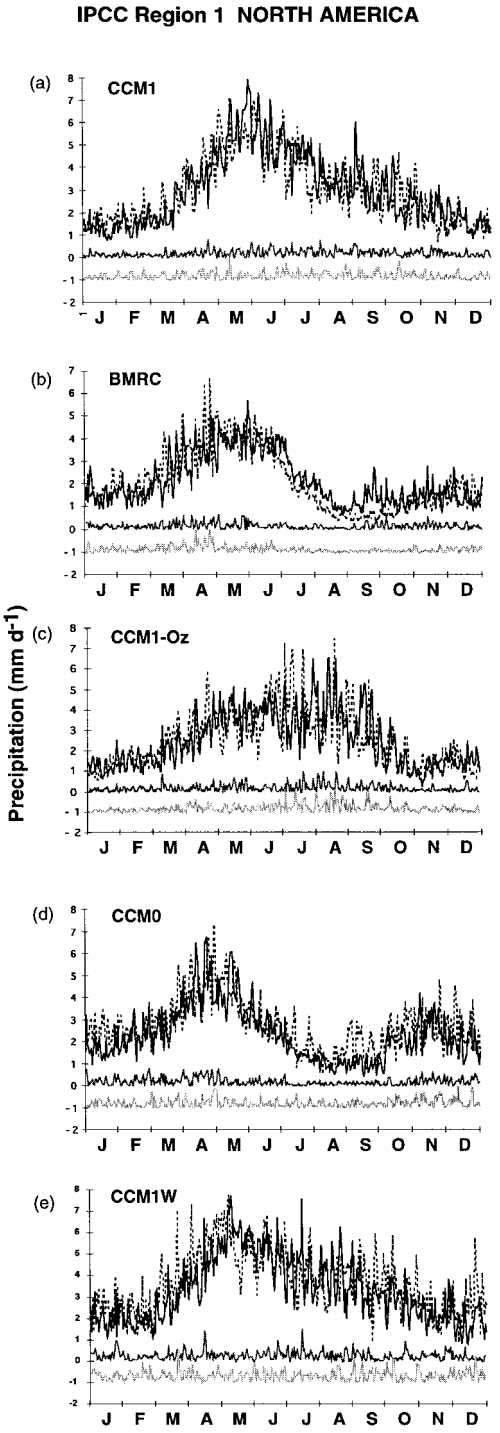

Figure 7. Seasonal cycle of precipitation and precipitation variability for $1\times$ and $2\times CO_2$ for CCM1Oz, BMRC, CCMlW, CCM1, CCM0, control run (upper, dotted) and perturbed run (upper solid) together with the magnitude of the Laplacian for control (dark lower) and perturbation (light lower displaced by -1), for North America

particularly at the higher precipitation values, there is a strong indication that regional precipitation events will shift to be more intense. There is considerable variation between models and some models show no notable change in some regions (e.g. CCM0 in Region 2, South Asia). For almost all models and all regions, the perturbed run shows more extreme events (high precipitation) than the control run and in general, return periods decrease. The relative change in return periods increases for less frequent events. This is in agreement with the findings of Gordon *et al.* (1992) and Whetton *et al.* (1993), but is contrary to the findings of Parey (1994). The short length of the data sequence results in some spurious high values of the return period ratio.

Figure 10 shows the change in precipitation distribution for the five IPCC regions. The abscissa shows the deciles, and the ordinate shows the change from control to enhanced-greenhouse climate. An overall increase in precipitation would, therefore, be indicated by a positive value at all deciles. Most of the regions reflect the overall global increase in precipitation. Notable exceptions are in Region 2, where the differences are negative for low precipitation amounts and positive for large precipitation amounts as would be expected for a simple change in variability. For Region 4 (Southern Europe), two models show a decrease in precipitation at all amounts (also indicated in Table III). There is a general consensus, echoing the results presented in Figure 9, that the amount of rain which is due to heavy precipitation events increases, although most of the models predict an increase at all intensities with a profile consistent with both change in mean and change in variability. Regional studies (Karl and Knight, 1998) are only beginning to reveal the complexity of regional scale variability and modeling studies must proceed in conjunction with observational studies for both validation and improved understanding of the processes involved.

Table II. Mean absolute magnitude of 'variability' for control and enhanced greenhouse conditions together with another measure of variability change, the fractional change of the S.D., σ, given in Table III, under enhanced greenhouse conditions from the five GCMs considered in this study

	CCM1Oz	BMRC	CCM1W	CCM1	CCM0
Region 1	(North America)				
Control	0.204	0.167	0.271	0.201	0.200
Perturbation	0.224	0.148	0.336	0.197	0.336
$\sigma 2\times/\sigma$	1.068	0.927	1.107	0.911	0.945
Region 2	(South Asia)				
Control	0.214	0.090	0.197	0.231	0.232
Perturbation	0.272	0.096	0.272	0.245	0.219
$\sigma 2\times/\sigma$	1.204	1.058	1.255	1.038	0.901
Region 3	(The Sahel)				
Control	0.107	0.049	0.199	0.166	0.122
Perturbation	0.126	0.051	0.240	0.159	0.149
$\sigma 2\times/\sigma$	1.102	1.018	1.055	0.918	0.960
Region 4	(Southern Europe)				
Control	0.070	0.040	0.131	0.103	0.095
Perturbation	0.076	0.040	0.152	0.100	0.117
$\sigma 2\times/\sigma$	1.135	1.125	1.049	0.919	1.232
Region 5	(Australia)				
Control	0.079	0.052	0.145	0.111	0.130
Perturbation	0.089	0.051	0.165	0.116	0.144
$\sigma 2\times/\sigma$	1.077	0.891	1.069	1.005	1.108

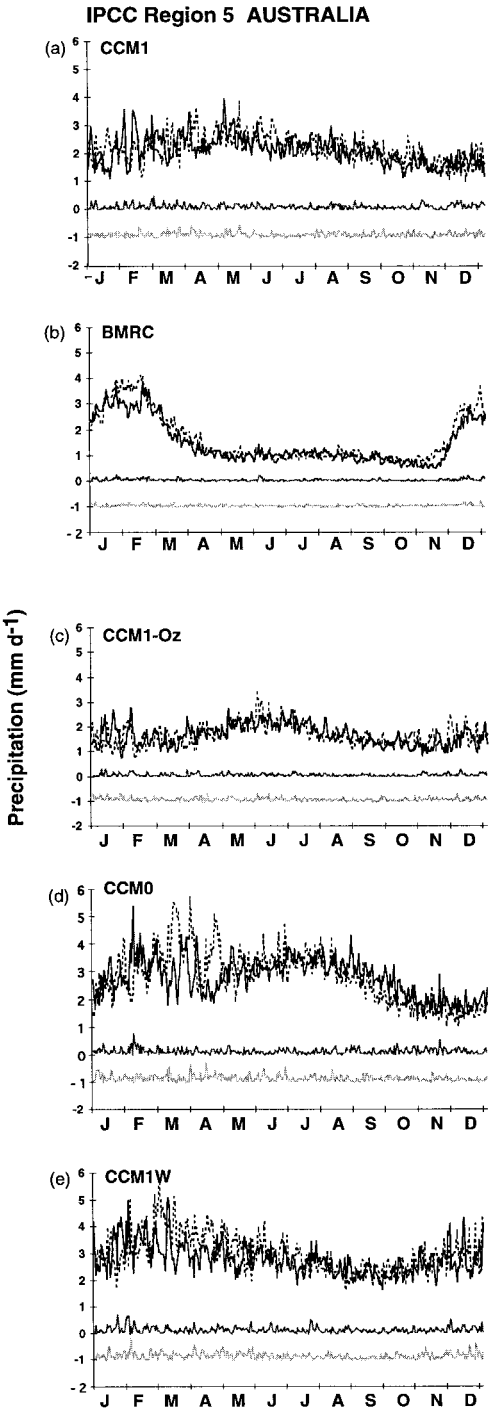

Figure 8. As for Figure 7, but for Australia

5.2. *Mean, variability, intensity and 'spells' of extremes*

Using the archived daily data, descriptive statistics about each models' regional precipitation characteristics have been calculated (Table III). The variables are the mean and S.D., the number of rain-days per year and the rain per rain-day, the name of the month with the maximum and minimum amount of

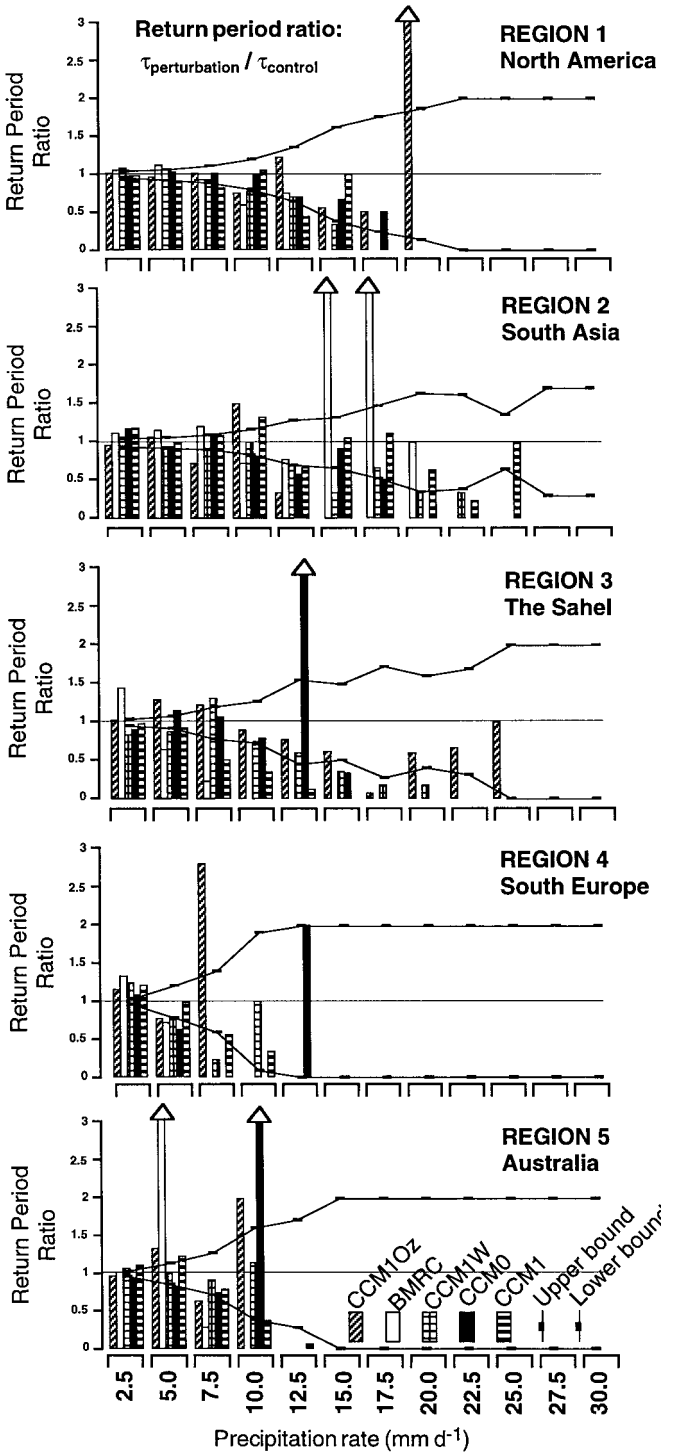

Figure 9. Return period changes for precipitation events of specified intensity (mm day^{-1}). Error bounds are derived from Equation (1) based on the mean number of events in each bin from all models

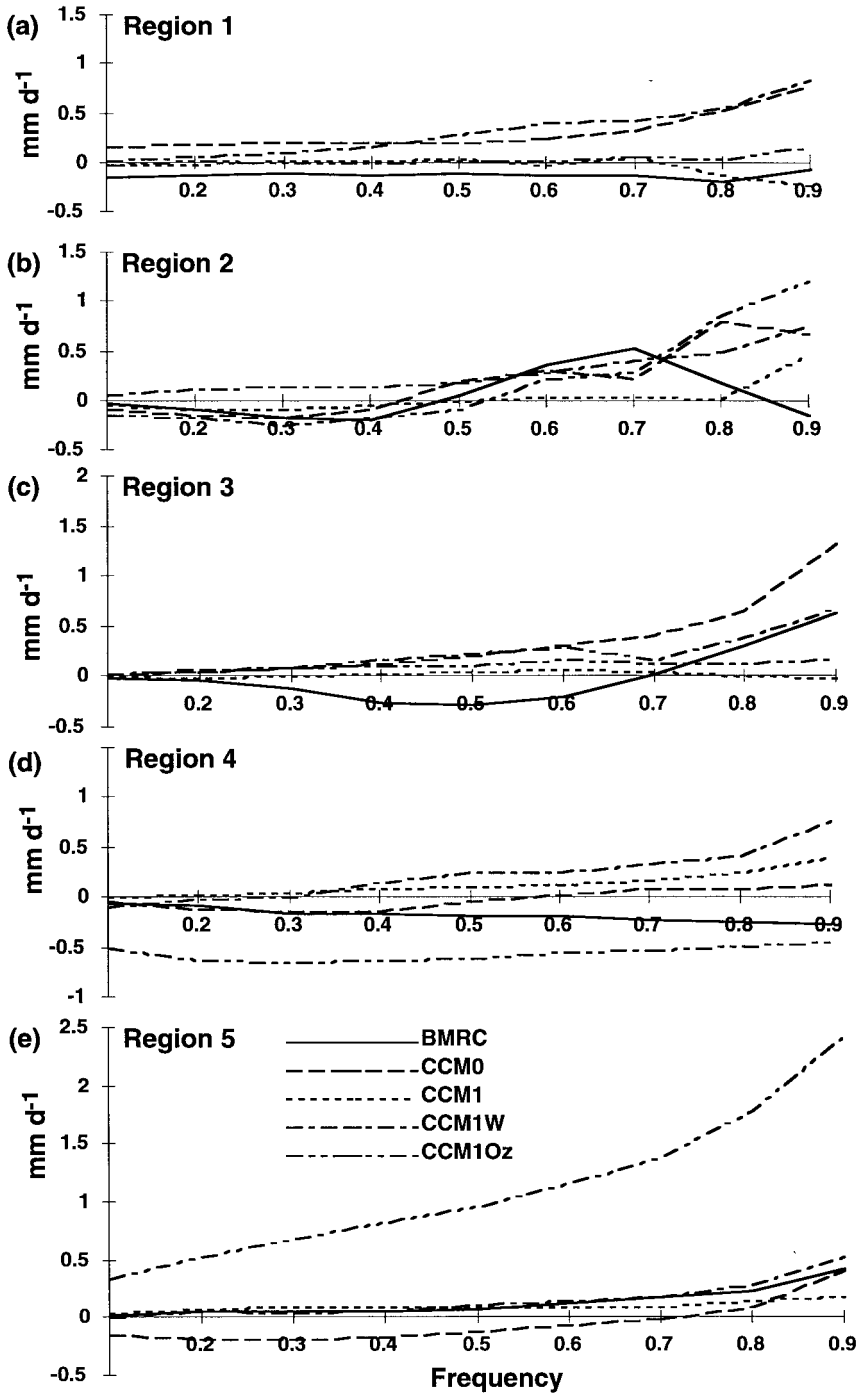

Figure 10. Changes in the cumulative frequency distribution for precipitation for enhanced CO_2 conditions

precipitation and the amount of precipitation in those months. A rain-day is defined as follows: if the precipitation in a grid-box is over 0.1 mm day^{-1}, it is considered to rain in that grid-box. The number of rain-days in a region is the fractional surface of the raining grid-boxes in the region. So if there is more than 0.1 mm day^{-1} of precipitation in the grid-boxes covering half the surface of a region it is considered

half a rain-day. Rain per rain-day is then the area averaged precipitation over the grid-boxes with more than 0.1 mm day^{-1}.

In every region (with the exception of North America (Region 1)) the majority of the models predict an increase in the mean. They also predict an increase in the variability, i.e. S.D. The increase in S.D. together with the increase in the mean causes more extreme precipitation events. All models predict an increase in mean precipitation (largely convective rainfall) in the tropical regions IPCC 2 (South Asia) and IPCC 3 (the Sahel). The change in the number of rain-days is, however, not the same in every region. In IPCC 2 (South Asia), all of the five models predict an increase in the number of rain-days, but in IPCC 4 (Southern Europe) they all predict a decrease. The intensity (rain per rain-day) increases in IPCC 4 according to all the models and two out of five in IPCC 2. In Southern Europe there is an increase in dry days, but when it rains the rain is more intense. This last point is in agreement with Noda and Tokioka (1989), who found a decrease in large scale stratiform rainfall and with Gordon *et al.* (1992) who found a decrease in rain-days over southern Europe. Rowntree *et al.* (1993) also found an increase in rainfall intensity in Europe. The models do not agree on whether this results in more or less average rainfall. In South Asia average rainfall and the number of rain-days increase but here the models show no agreement in the change of intensity. Four models predict an increase in the number of rain-days in IPCC 3 and 5 (Australia).

As well as considering frequency and intensity of extreme precipitation by investigating the return period of extreme events and the number of rain-days, it is valuable to look at the persistence of extreme dry and wet days. There is only a weak relationship between periods of low precipitation and droughts. The World Meteorological Organisation (Hounam *et al.*, 1975) gives several definitions of droughts or, better, dry spells, solely based on rainfall. These definitions have in common that they define a dry spell as a period with precipitation below a certain threshold. The definition used here for a dry spell is a period of 7 days with precipitation on each day less than the first decile. To calculate the dry and wet spells for the perturbed run, the first and ninth decile of the control run are used.

Table IV shows the number of dry and wet spells together with their average duration and the average amount of precipitation during that period for each model in every region for the control and perturbed run. The first and ninth decile are also shown in the table. Note that the dry and wet spells in the perturbed run are based on the first and ninth decile of the control run. Except for IPCC 3 (the Sahel) the models predict decrease in the first decile, indicating more days with little or no rainfall. In the Sahel, the modeled climate shows fewer extreme dry days. This is backed by the results shown in Table III, which indicate an increase in the number of rain-days in the Sahel. The value for the first decile in the Sahel is still, however, an order of magnitude less than in the other regions meaning that it remains a very dry area with a high seasonality of rainfall in these model simulations.

Even though in the results for the Sahel from most of the models the first decile increases, none of the models predict fewer dry spells. The ninth decile increases in every region according to the majority of the models. It is a representation of the increase in mean and S.D., found in Table III. This means more extreme wet days and possibly more wet spells. The number of wet spells increases overall but it is not clearly shown for all the models in every region. In Southern Europe (IPCC 4) the models predict more dry spells. In view of the fact that the models predict fewer rain-days, this was to be expected. The increase in intensity occurs along with an increase in the number of wet spells. In the North American (IPCC 1) and Australian (IPCC 5) regions, the models do not agree with each other about the increase or decrease of wet and dry spells (Table II). In Australia however, four models indicate longer lasting wet spells in the perturbed climate (Figure 10). The increase in variability, makes a day with extreme dry or wet weather more probable and could therefore lead to more dry and wet spells. The small numbers of dry spells means that changes in their frequency will be very hard to detect reliably. The monsoon in Region 2 causes a large number of wet spells, because the extreme rainfall events all occur within a season. Whether or not the modeled dry and wet spells are more severe, last longer and are drier or wetter in general cannot be concluded from these numbers. However, there are more wet spells in the tropics, South Asia (IPCC2) and the Sahel (IPCC3) and an increase in dry spells over southern Europe (IPCC4). A relatively short period of data (10 years) has been investigated here from five different models whereas

Table III. Descriptive statistics for precipitation in the five IPCC regions

	CCM1Oz		BMRC		CCM1W		CCM1		CCM0	
	Cont	Pert	Cont	Pert	Cont	Pert	Cont	Pert	Cont	Pert
IPCC 1	North America									
Mean	2.52	2.59	2.24	2.14	3.22	3.59	2.88	2.87	2.34	2.70
σ	2.69	2.88	1.88	1.98	2.77	3.18	2.47	2.51	2.18	2.50
Rain-days/year	207.32	200.28	247.20	238.44	180.00	180.44	222.84	214.68	169.44	202.80
Rain/rain-day	7.79	8.52	4.58	4.43	13.48	15.77	7.70	8.51	7.67	8.61
Maximum m	August	July	May	May	May	July	May	May	May	April
Maximum Pr	180.85	171.93	148.23	166.94	214.12	206.15	196.00	196.02	170.69	189.44
Minimum m	November	November	August	September	February	November	February	January	September	August
Minimum pr	20.21	21.84	17.38	9.05	38.42	37.44	28.18	37.20	12.67	23.84
IPCC 2	South Asia									
Mean	5.38	5.68	4.77	4.81	3.49	3.84	3.57	3.65	5.93	6.16
σ	3.96	4.67	4.73	4.77	3.25	3.60	2.89	3.18	5.23	5.84
Rain-days/year	228.12	230.76	189.48	189.48	141.96	144.60	170.16	171.00	204.40	205.32
Rain/rain-day	12.94	12.96	12.04	11.74	20.02	21.54	16.16	15.91	15.34	15.34
Maximum m	August	October	July	June	July	July	September	August	July	August
Maximum pr	357.41	313.61	380.35	364.86	258.73	329.46	255.61	254.09	548.92	632.64
Minimum m	March	January	January	March	March	March	April	April	February	March
Minimum pr	43.40	27.69	2.75	2.41	11.67	17.65	22.33	19.21	16.62	16.93
IPCC 3	The Sahel									
Mean	1.75	1.87	1.74	1.78	2.45	2.80	1.60	1.67	1.77	2.25
σ	2.11	2.20	1.51	1.79	2.45	2.80	1.60	1.67	1.77	2.25
Rain-days/year	123.48	127.80	158.40	155.04	98.40	102.84	100.56	102.60	131.64	146.40
Rain/rain-day	11.37	11.92	6.96	6.95	24.84	27.08	15.91	15.85	12.00	11.77
Maximum m	August	October	August	August	August	July	July	July	July	July
Maximum pr	167.21	148.62	165.67	161.91	258.17	295.66	144.25	225.63	163.1	224.78
Minimum m	December	January	February	January	January	February	February	February	January	January
Min pr	2.15	1.97	1.58	0.78	2.93	4.06	2.79	1.85	11.29	7.26
IPCC 4	South Europe									
Mean	2.01	1.93	1.44	1.28	2.65	2.93	2.46	2.60	2.50	2.50
σ	1.00	1.07	0.94	0.84	1.43	1.77	1.05	1.17	1.41	1.51
Rain-days/year	234.0	223.68	192.00	177.48	180.00	177.12	233.52	231.00	204.96	192.48
Rain/rain-day	4.91	5.16	5.97	6.39	12.14	13.60	6.15	6.69	8.72	9.90
Maximum m	December	March	January	April	November	December	October	January	January	January
Max pr	110.11	108.25	85.43	72.73	136.93	159.66	113.04	121.01	131.45	136.08
Minimum m	July	July	July	July	August	August	August	August	August	August
Minimum pr	22.86	14.90	5.52	4.49	15.56	12.70	12.68	12.20	16.97	15.96

Table III. (continued)

	CCM1Oz		BMRC		CCM1W		CCM1		CCM0	
	Cont	Pert	Cont	Pert	Cont	Pert	Cont	Pert	Cont	Pert
IPCC 5	Australia									
Mean	1.74	1.82	1.59	1.75	2.93	3.12	2.24	2.33	3.00	3.00
σ	1.04	1.09	1.15	1.32	1.59	1.84	1.25	1.26	1.64	1.88
Rain-days/year	180.96	180.48	152.16	155.16	151.32	153.84	170.40	173.40	182.4	183.24
Rain/rain-day	7.34	7.44	8.49	8.90	17.90	18.17	10.46	10.48	11.18	11.79
Maximum m	March	December	January	January	February	March	May	February	March	March
Maximum pr	88.95	86.07	118.90	164.51	153.68	217.45	119.43	127.40	165.75	191.76
Minimum m	February	October	October	October	August	August	October	November	December	November
Minimum pr	30.53	27.82	17.94	20.26	54.40	55.20	39.27	38.74	37.69	34.00

Statistics include: mean, S.D. (σ); rain-days per year; rain per rain-day; month of maximum (maximum m); average maximum precipitation in that month (maximum pr); month of minimum precipitation (minimum m); and average minimum in that month (minimum pr); cont—control; pert—perturbed.

Table IV. Dry and wet spells for each of the five regions named in the text

	CCM1Oz		BMRC		CCM1W		CCMI		CCM0	
	Cont	Pert	Cont	Pert	Cont	Pert	Cont	Pert	Cont	Pert
IPCC 1	North America									
Decile 1	0.41	0.39	0.52	0.38	0.74	0.67	0.67	0.65	0.38	0.55
Dry										
Number	0	5	5	15	2	2	1	0	7	3
Duration	—	7.40	7.80	10.61	7.50	8.00	10.00	—	8.57	7.0
Precipitation	—	1.76	2.27	2.93	2.35	2.12	3.24	—	1.44	1.30
Decile 9	5.80	6.07	4.78	4.71	7.09	7.93	6.40	6.24	5.13	5.90
Wet										
Number	2	0	0	0	0	0	0	1	0	1
Duration	7.50	—	—	—	—	—	—	8.00	—	7.00
Precipitation	66.12	—	—	—	—	—	—	72.46	—	45.51
IPCC 2	South Asia									
Decile 1	1.31	1.15	0.14	0.11	0.49	0.54	0.74	0.69	0.91	0.62
Dry										
Number	6	14	11	21	8	3	5	3	11	10
Duration	9.50	9.21	10.18	9.62	7.63	9.33	8.60	7.00	8.73	9.10
Precipitation	6.99	6.72	0.61	0.59	1.91	2.05	3.46	2.69	3.04	3.29
Decile 9	11.25	12.46	11.81	11.64	8.07	8.84	7.62	8.09	14.52	15.19
Wet										
Number	10	13	15	11	8	9	3	5	8	14
Duration	8.10	10.54	9.27	8.18	9.25	9.11	7.67	7.80	10.88	10.87
Precipitation	122.70	176.62	134.07	116.70	111.64	124.29	88.18	97.16	204.51	202.31
IPCC 3	The Sahel									
Decile 1	0.06	0.08	0.08	0.06	0.05	0.08	0.03	0.05	0.1	0.22
Dry										
Number	6	6	13	18	2	6	4	7	1	3
Duration	12.50	8.00	10.84	11.56	7.00	7.83	15.25	8.71	7.00	7.00
Precipitation	0.29	0.17	0.33	0.30	0.10	0.10	0.26	0.17	0.32	0.57
Decile 9	4.78	4.96	3.86	4.46	7.01	7.67	4.43	4.41	4.20	5.54
Wet										
Number	9	3	10	31	4	8	4	5	6	18
Duration	9.89	7.67	13.60	11.90	8.75	7.25	8.25	9.80	8.17	11.67
Precipitation	70.57	57.70	69.24	67.53	97.31	88.52	59.60	81.62	57.15	92.84
IPCC 4	South Europe									
Decile 1	0.78	0.67	0.23	0.17	0.84	0.73	1.17	1.18	0.67	0.64
Dry										
Number	9	12	12	20	16	17	4	5	13	13
Duration	10.00	10.00	10.67	9.45	10.06	11.12	16.75	16.40	8.77	9.38
Precipitation	5.12	4.57	1.30	1.06	3.86	4.48	9.73	10.51	2.78	2.72
Decile 9	3.35	3.37	2.71	2.45	4.52	5.28	3.81	4.20	4.40	4.52
Wet										
Number	3	2	5	5	0	8	0	5	0	3
Duration	8.33	7.50	7.40	8.40	—	7.88	—	7.60	—	9.00
Precipitation	34.46	34.73	24.58	28.96	—	48.86	—	37.95	—	51.39

Table IV. (continued)

	CCM1Oz		BMRC		CCM1W		CCMI		CCM0	
	Cont	Pert	Cont	Pert	Cont	Pert	Cont	Pert	Cont	Pert
IPCC 5	Australia									
Decile 1	0.78	0.75	0.55	0.58	1.40	1.41	1.02	1.06	1.27	1.12
Dry										
Number	3	8	3	0	0	1	2	1	3	1
Duration	7.33	7.75	8.00	—	—	7.00	7.00	7.00	9.67	8.00
Precipitation	3.69	4.25	3.11	—	—	7.26	5.13	5.82	7.90	6.88
Decile 9	3.08	3.13	3.24	3.66	5.06	5.59	3.69	3.87	5.11	5.51
Wet										
Number	4	2	14	21	3	9	3	3	1	12
Duration	7.00	8.00	11.14	14.19	7.67	8.67	8.33	8.67	10.00	8.83
Precipitation	35.64	37.27	51.76	68.39	55.53	67.37	49.88	52.66	78.99	59.85

Table shows values of first and ninth deciles together with (for both wet and dry spells) average duration of dry/wet spell, number of dry/wet spells (in 10 year period) and amount of precipitation (precip) during the dry/wet spell; cont—control; pert—perturbed.

Whetton *et al.* (1993) analyzed 28 years of data from one model. The use of more than one model offers an estimate of confidence based on the level of model agreement rather than on statistical analysis of the single model results.

The largest changes occur in the tropics. Gordon *et al.* (1992) finds an increase in convective rainfall in the CSIRO model, resulting in shorter return periods for extreme events and an increase in the intensity of the rainfall. This study also suggests a decrease in return period in all five IPCC regions. In addition, the MECCA models exhibit an increase in intensity in most regions except IPCC 2 (South Asia). In South Asia, however, there is an increase in the number of rain-days and in the number of wet spells. The number of rain-days decreases in IPCC 4 (Southern Europe). In general, there is an increase in the mean and variability of precipitation, a decrease in return period of extreme events and an increase in intensity and the number of wet spells. This is again in agreement with the results of some researchers (Gordon *et al.*, 1992; Whetton *et al.*, 1993) but contrasts with the results of Parey (1994).

6. SUMMARY AND CONCLUSIONS

Although the five selected MECCA models have some common parentage, there are many differences in their parameterizations and some differences in resolution. The experiments compared also differ. All those compared here are instantaneous enhanced greenhouse simulations and all employ simple mixed-layer ocean models. However, as described above, the types of greenhouse enhancement used differ, as do the lengths of simulations. It is very important to note the differences in initial conditions and in the scenarios of enhanced greenhouse conditions used in these simulations: most modelers have simply doubled the concentration of CO_2 from the control case to achieve the enhanced greenhouse scenario. However, this is not the case for CCM1 or CCM1W simulations (Table I) and none of the simulations take account of the possible impact of sulphate aerosols.

The aim of this analysis has been to examine ways in which we can determine our confidence in computer model predictions of climate variability under enhanced CO_2 conditions. This paper offers some insight into the extent to which variability of regional climate differs among this suite of models. It is valuable to review these results in conjunction with the detailed evaluation of the performance of other GCMs in, for example, Houghton *et al.* (1990, 1996) and Santer *et al.* (1990).

A number of measures of variability have been examined and all of the models show an increase in variability at the global scale as measured by the S.D. of temperature and precipitation. The results show less agreement at a regional scale and examination of the variability of the IPCC regions has shown important differences in the response of the different models to the CO_2 perturbation at a regional scale and also has shown important differences in the temporal distribution of that 'variability' across the seasons. This analysis has shown that the use of a single model to determine regional and continental scale variability changes is likely to be prone to error. Although the models behave reasonably consistently on an annual timescale, there are significant differences at a seasonal timescale and intermodel differences tend at least to match if not exceed, changes due to enhanced greenhouse gases. Any temporal shift in periods of high variability is likely to be important at a regional scale, since agricultural techniques tend to have an unevenly distributed tolerance. Analysis of the distribution of return periods has shown that although the models agree reasonably well at a global scale, with relative positions of major atmospheric circulation features being reasonable, the changes experienced in a region will be crucially dependent on the positioning and strength of that feature and its response to enhanced CO_2. It seems that although global climate models may be said from this study to agree reasonably on the response of the global atmosphere to enhanced CO_2, the regional scale changes cannot be directly inferred from the model results without closer interpretation of the physical processes, particularly the level of verisimilitude relevant processes in the control simulation.

ACKNOWLEDGEMENTS

This research was funded in part by grants from the Model Evaluation Consortium for Climate Assessment, the Department of the Environment, Sport and Territories and by the Australian Research Council. Ann-Maree Hansen contributed to an earlier version of this paper.

REFERENCES

Brown, B.G. and Katz, R.W. 1995. 'Regional analysis of temperature extremes: Spatial analog for climate change?', *J. Climate*, **8**, 108–119.

Dickinson, R.E., Henderson-Sellers, A., Kennedy, P.J. and Giorgi, F. 1992. *Biosphere Atmosphere Transfer Scheme (BATS)*, version le as coupled to the NCAR community climate model, NCAR Tech Note, National Center for Atmospheric Research, Boulder, CO.

Fowler, A.M. and Hennessey, K.J. 1995. 'Potential impacts of global warming on the frequency and magnitude of heavy precipitation', *Nat. Hazards*, **11**, 283–303.

Gates, W.L. 1992. 'AMIP: The atmospheric model intercomparison project', *Bull. Am. Meteorol. Soc.*, **73**, 1962–1970.

Giorgi, F. and Mearns, L.O. 1991. 'Approaches to the simulation of regional climate charge: a review', *Rev. Geophys.*, **29**, 191–216.

Gordon, H.B., Whetton, P.H., Pittock, A.B., Fowler, A.M. and Haylock, M.R. 1992. 'Simulated changes in daily rainfall intensity due to the enhanced greenhouse effect: implications for extreme rainfall events', *Clim. Dyn.*, **8**, 83–102.

Hart, T.L., Bourke, W., McAvaney, B.J., Forgan, B.W. and McGregor, J.L. 1990. 'Atmospheric general circulation simulations with the BMRC global spectral model: the impact of revised physical parameterizations', *J. Climate*, **3**, 436–459.

Henderson-Sellers, A. and Hansen, A. 1995. *Climate Change Atlas: Greenhouse Simulations from the Model Evaluation Consortium for Climate Assessment*, Kluwer Academic, Dordrecht, 159 pp.

Henderson-Sellers, A., Dickinson, R.E., Durbidge, T.B., Kennedy, P.J., McGuffie, K. and Pitman, A.J. 1993. 'Tropical deforestation: modelling local to regional scale climate change', *J. Geophys. Res.*, **98**(D4), 7289–7315.

Henderson-Sellers, A., Howe, W. and McGuffie, K. 1995. 'The MECCA analysis project, 1995', *Glob. Planet. Change.*, **10**, 3–21.

Henderson-Sellers, A., Zhang, H., Berz, G., Emanuel, K., Gray, W., Landsea, C., Holland, G., Lighthill, J., Shieh, S-L., Webster, P. and McGuffie, K. 1998, 'Tropical cyclones and climate change: A post IPCC assessment', *Bull. Am. Meteorol. Soc.*, **79**, 19–38.

Hennessey, K.J. and Pittock, A.B. 1995. 'Greenhouse warming and threshold temperature events in Victoria, Australia', *Int. J. Climatol.*, **15**, 591–612.

Hennessey, K.J., Fowler, A.M. and Whetton, P.H. 1993. 'GCM simulated changes in daily rainfall intensity and heavy rainfall events under an enhanced greenhouse effect', in *Preprints of the Fourth International Conference on Southern Hemisphere Meteorology and Oceanography*, Hobart, Australia, American Meteorological Society, Boston, MA, pp. 199–200.

Houghton, J.T., Jenkins, G.J. and Ephraums, J.J. 1990. *Climate Change The IPCC Scientific Assessment*, Cambridge University Press, 364 pp.

Houghton, J.T., Callander, B.A. and Varney, S.K. 1992. *Climate Change 1992: The Supplementary Report to the IPCC Scientific Assessment*, Cambridge University Press, 112 pp.

Houghton, J.T., Miera Filho, L.G., Callander, B.A., Harris, N., Kattenberg, A. and Maskell, K. 1996. *Climate Change 1995. The Science of Climate Change: Contribution of Working Group I to the Second Assessment Report of the Intergovernmental Panel on Climate Change*, Cambridge University Press, Cambridge, 572pp.

Hounam, C., Burgos, J., Kalik, M., Palmer, W. and Rodda, J. 1975. *Drought and Agriculture*, World Meteorological Organisation, Technical Note No. 138, Geneva, Switzerland, 128pp.
Hu, Q., Woodruff, C.M. and Mudrick, S.E. 1998. 'Interdecadal variations of annual precipitation in the Central United States', *Bull. Am. Meteorol. Soc*., **79**, 221–229.
Karl, T.R. and Knight, R.W. 1998. 'Secular trends of precipitation amount, frequency and intensity in the United States', *Bull. Am. Meteorol. Soc*., **79**, 233–241.
Katz, R.W. and Brown, B.G. 1992. 'Extreme events in a changing climate: variability is more important than averages', *Clim. Change*, **21**, 289–302.
Kuo, H.L. 1974. 'Further studies of the parameterization of the influence of cumulus convection on large scale flow', *J. Atmos. Sci*., **31**, 1232–1240.
Legates, D.R. and Willmott, C.J. 1990a, 'Mean seasonal and spatial variability in gauge-corrected global precipitation', *Int. J. Climatol*., **10**, 111–127.
Legates, D.R. and Willmott, C.J. l990b. 'Mean seasonal and spatial variability in global surface air temperature', *Theor. Appl. Climatol*., **41**, 11–21.
Lighthill, J., Holland, G.J., Gray, W.M., Landsea, C., Emanuel, K., Craig, G., Evans, J., Kuhihara, Y. and Guard, C.P. 1994. 'Global climate change and tropical cyclones', *Bull. Am. Meteorol. Soc*., **75**, 2147–2157.
Manabe, S., Smagorinsky, J. and Strickler, R.F. 1965. 'Simulated climatology of a general circulation model with a hydrological cycle', *Mon. Wea. Rev*., **93**, 769–798.
Mearns, L.O., Giorgi, F., McDaniel, L. and Shields, C. 1995a. 'Analysis of daily variability in precipitation in a nested regional climate model: comparison with observations and doubled CO_2 results', *Glob. Planet. Change*, **10**, 55–78.
Mearns, L.O., Giorgi, F., McDaniel, L. and Shields, C. 1995b. 'Analysis of the diurnal range and variability of daily temperature in a nested modelling experiment: comparison with observations and doubled CO_2 results', *Clim. Dyn*., **11**, 193–209.
Noda, A. and Tokioka, T. 1989. 'The effect of doubling the CO_2 concentration on convective and non-convective precipitation in a general circulation model coupled with a simple mixed layer ocean model', *J. Meteorol. Soc. Jpn*., **67**, 1057–1069.
Oglesby, R. and Saltzman, B. 1992. 'Equilibrium climate statistics of a GCM as a function of atmospheric CO_2 Part I', *J. Climate*, **5**, 66–92.
Parey, S. 1994, *Simulations de Trente Ans 1 × CO_2, 2 × CO_2, 3 × CO_2 avec le Modele du LMD (64 × 50 × 11) Premiers Resultats*, EDF, Direction des Etudes et Recherches, HE-33/94/009.
Penner, J. and Taylor, K.E. 1994, 'Responses of the climate system to atmospheric aerosols and greenhouse gases', *Nature*, **369**, 734–737.
Roeckner, E. and von Storch, H. 1980. 'On the efficiency of horizontal diffusion and numerical filtering in an Arakawa-type model', *Atmosphere–Ocean*, **18**, 239–253.
Rowntree, P.R., Murphy, J.M., Mitchell, J.F.B. 1993. 'Climatic change and future rainfall predictions', *J. Inst. Water Environ. Mgmt*, **7**, 464–470.
Santer, B.D., Wigley, T.M.L., Schlesinger, M.E. and Mitchell, J.F.B. 1990. *Developing Climate Scenarios from Equilibrium GCM Results*, Max Planck Institut fur Meteorologie, Report No., 47, Hamburg, Germany, 29 pp.
Tegart, W.J. McG., Sheldon, G.W. and Griffiths, D.C. 1990, *Climate Change. The IPCC Impacts Assessment*, report prepared by Working Group II for the Intergovernmental Panel on Climate Change, Australian Government Printing Service, Canberra, Australia, 312 pp.
Tiedtke, M. 1984. 'The effect of penetrative cumulus convection on the large scale flow in a general circulation model', *Beitr. Phys. Atmos*., **57**, 216–239.
Wang, W-C, Dudek, M.D. and Liang, X. 1992. 'Inadequacy of effective CO_2 as a proxy to assess the greenhouse effect of other radiative gases', *Geophys. Res. Lett*, **19**, 1375–1378.
Washington, W.M. and Meehl, G. 1992, 'Greenhouse sensitivity experiments with penetrative cumulus convection and tropical cirrus albedo effects', *Clim. Dyn*., **8**, 211–233.
Whetton, P.H., Fowler, A.M., Haylock, M.R. and Pittock, A.B. 1993. 'Implications of climate change due to the enhanced greenhouse effect on floods and droughts in Australia', *Clim. Change*, **25**, 289–317.

